Electronic Supplementary Information

Aggregation-Induced Emission Luminogen with Excellent Triplet-Triplet Upconversion Efficiency for Highly Efficient Non-Doped Blue Organic Light-Emitting Diode

Pengbo Han,[a] Chengwei Lin,[a] Kaojin Wang,[a] Yanping Qiu,[a] Haozhong Wu,[a] Anjun Qin,[a,*] Dongge Ma,[a,*] and Ben Zhong Tang[a,b,*]

[a.] State Key Laboratory of Luminescent Materials and Devices, Guangdong Provincial Key Laboratory of Luminescence from Molecular Aggregates, Center for Aggregation-Induced Emission, South China University of Technology, Guangzhou, Guangdong 510640, China.

[b.] Shenzhen Institute of Molecular Aggregate Science and Engineering, School of Science and Engineering, The Chinese University of Hong Kong, Shenzhen, 2001 Longxiang Boulevard, Longgang District, Shenzhen City, Guangdong 518172, China.

Materials and Instruments

All the chemicals and reagents were purchased from commercial sources and used as received without further purification. ^{1}H and ^{13}C NMR spectra were measured on a Bruker AV 500 spectrometer in deuterated dichloromethane. High resolution mass spectra (HRMS) were recorded on a GCT premier CAB048 mass spectrometer operating in MALDI-TOF mode. TGA analysis was carried out on a TA TGA Q5000 and DSC analysis was performed on a DSC Q1000 under dry nitrogen at a heating rate of 10 ^{o}C min^{-1}. UV-vis absorption spectra were measured on a Shimadzu UV-2600 spectrophotometer. Photoluminescence spectra were recorded on a Horiba Fluoromax-4 spectrofluorometer. Fluorescence quantum yields were measured using a Hamamatsu absolute PL quantum yield spectrometer C11347 Quantaurus_QY. Fluorescence lifetimes were determined with a Hamamatsu C11367-11 Quantaurus-Tau time-resolved spectrometer. The frontier orbitals of the molecules based on the ground state geometries were calculated at B3LYP/6-31G (d,p) by Gaussian 09 program. Cyclic voltammetry (CV) were performed on a CHI 610E A14297 in a solution of tetra-*n*-butylammonium hexafluorophosphate (Bu_4NPF_6) (0.1 M) in dichloromethane (DCM) or dimethylformamide (DMF) at a scan rate of 100 mV s^{-1}, using a platinum wire as the auxiliary electrode, a glass carbon disk as the working electrode and Ag/Ag+ as the reference electrode. HOMO = − [E_{ox} − $E_{1/2}(Fc/Fc^{+})$ + 4.8] eV, LUMO = − [E_{red} − $E_{1/2}(Fc/Fc^{+})$ + 4.8] eV, where E_{ox} and E_{red} represent the onset oxidation potential and the reduction potential relative to Fc/Fc^{+} (4.8 eV), respectively, and $E_{1/2}$ (Fc/Fc^{+}) represents the calibrated value.

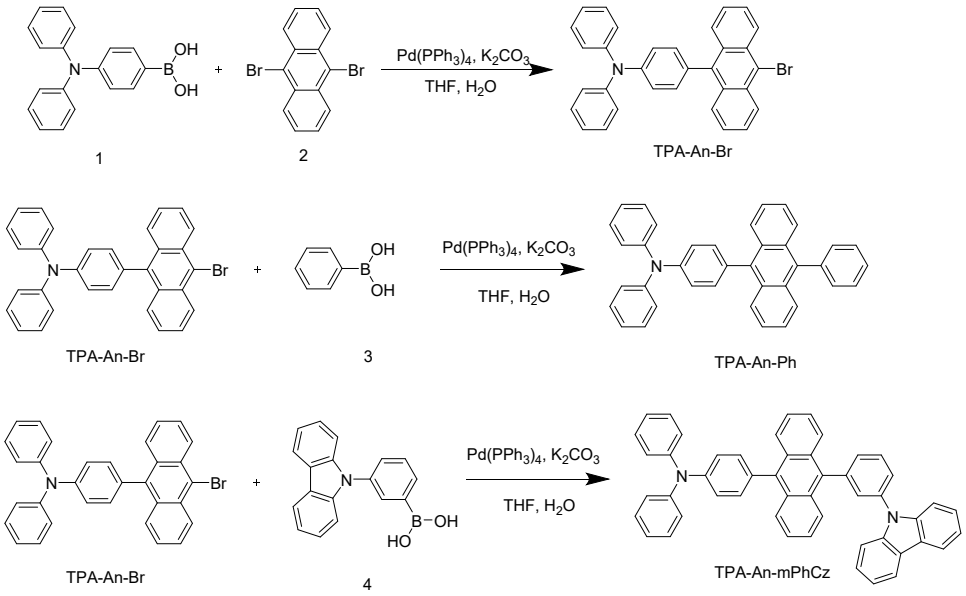

Scheme S1 Synthetic routes to TPA-An-Ph and TPA-An-mPhCz.

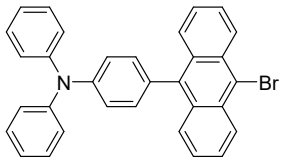

TPA-An-Br

Synthesis of 4-(10-bromoanthracen-9-yl)-N,N-diphenylaniline (TPA-An-Br**)**

Compound **1** (500 mg, 1.73 mmol), compound **2** (400 mg, 1.19 mmol), anhydrous potassium carbonate (492 mg, 3.57 mmol) and $Pd(PPh_3)_4$ (69 mg, 0.06 mmol) were added into a 100 ml two neck round bottom flask under N_2, then tetrahydrofuran (THF, 6 mL) and water (1 mL) was injected into the flask. The reaction solution was stirred at 74 ^oC for 6 h. After cooling to room temperature, the solution was poured into water and extracted with DCM for three times, and then organic phase was combined and dried over anhydrous magnesium sulfate. After filtration, the organic phase was concentrated by a rotary evaporator under reduced pressure, and the residue was purified by a silica gel column chromatography using PE/DCM (1:1 v/v) as eluent.

Yellow solid of TPA-An-Br was obtained in 81.0% (482 mg). ^{1}H NMR (500 MHz, CD_2Cl_2), δ (TMS, ppm): 9.32 (d, 1H), 8.55 (d, 1H), 8.34 (d, 1H), 8.17 (d, 1H), 8.06 (t, 2H), 7.97 (d, 4H), 7.87 (t, 1H). ^{13}C NMR (125 MHz, CD_2Cl_2), δ (TMS, ppm): 149.04, 148.81, 139.21, 133.23, 133.07, 132.54, 131.56, 130.68, 128.95, 128.81, 128.35, 126.81, 125.97, 124.49, 124.36, 123.51.

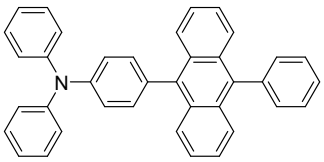

TPA-An-Ph

Synthesis of *N*,*N*-diphenyl-4-(10-phenylanthracen-9-yl)aniline (TPA-An-Ph)

TPA-An-Ph was obtatined according previous work.[1] ^{1}H NMR (500 MHz, CD_2Cl_2), δ (TMS, ppm): 7.84 (d, 2H), 7.61 (d, 2H), 7.58-7.54 (m, 3H), 7.46 (2H, d), 7.36-7.25 (16H, m), 7.08 (m, 2H). ^{13}C NMR (125 MHz, CD_2Cl_2), δ (TMS, ppm): 148.63, 148.04, 139.83, 137.18, 133.48, 132.88, 132.05, 130.14, 129.20, 127.76, 127.66, 125.34, 124.11, 123.83. HRMS ($C_{38}H_{27}N$): *m/z* 497.2137 (M+, calcd 497.2143).

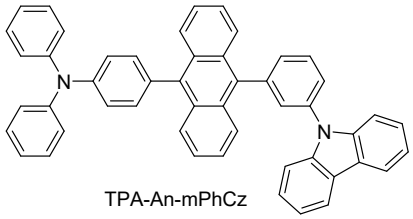

TPA-An-mPhCz

Synthesis of 4-(10-(3-(9H-carbazol-9-yl)phenyl)anthracen-9-yl)-N,N-diphenylaniline (TPA-An-mPhCz)

TPA-An-mPhCz was synthesized by similar procedures as TPA-An-Br from the reagents of **4** and TPA-An-Br in 86% yield. ^{1}H NMR (500 MHz, CD_2Cl_2), δ (TMS, ppm): 8.15 (d, 2H), 7.85-7.72 (m, 5H), 7.73 (t, 1H), 7.60 (m, 3H), 7.42 (m, 6H), 7.34-

7.26 (d, 13H), 7.09 (d, 2H). ^{13}C NMR (125 MHz, CD_2Cl_2), δ (TMS, ppm): 149.14, 148.63, 142.35, 142.05, 139.23, 138.83, 136.94, 133.39, 133.37, 131.60, 131.41, 131.34, 131.22, 130.87, 130.67, 128.46, 127.91, 127.32, 126.75, 126.38, 125.90, 124.75, 124.60, 124.59, 124.39, 121.54, 121.35, 111.16. HRMS ($C_{49}H_{34}N_2$): *m/z* 662.2729 (M+, calcd 662.2722).

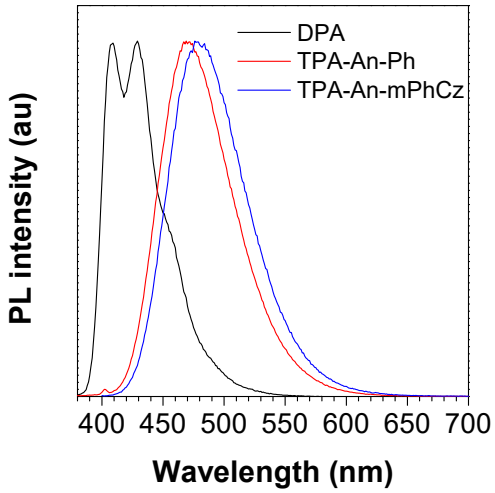

Fig. S1. PL spectra of DPA, TPA-An-Ph and TPA-An-mPhCz in THF soultions. λ_{ex}: 360 nm; concentration: 10 μM.

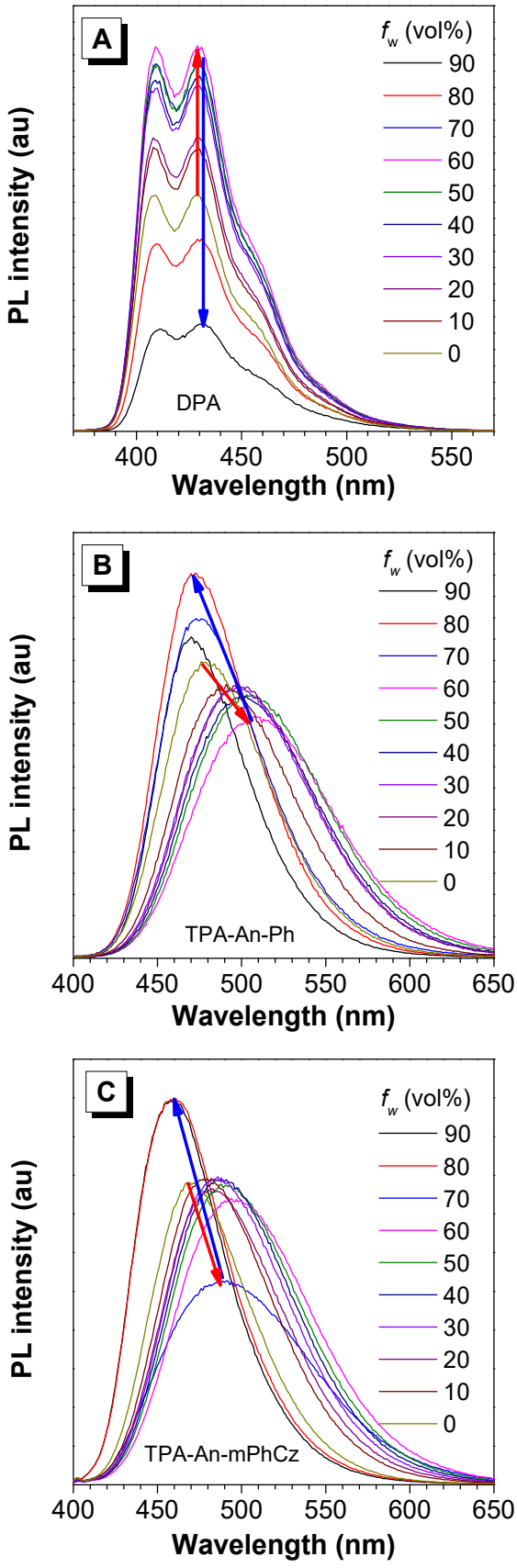

Fig. S2. PL spectra of (A) DPA, (B) TPA-An-Ph and (C) TPA-An-mPhCz in THF/water mixtures with different water fractions. λ_{ex}: 360 nm; concentration: 10 μM.

Table S1. Detailed absorption and emission peaks of DPA in different solvents

solvents	ε	n	$f(\varepsilon,n)$	λ_a [nm]	λ_f [nm]	ν_a-ν_f [cm^{-1}]
hexane	1.90	1.375	0	392	406	880
toulene	2.40	1.497	0.013	395	409	867
triethylamine	2.42	1.401	0.048	392	406	880
isopropyl ether	3.88	1.386	0.145	392	405	819
chloroform	4.80	1.446	0.148	396	411	921
ethyl acetate	5.10	1.372	0.200	392	406	880
tetrahydrofuran	7.58	1.407	0.210	395	409	867
dichloromethane	8.93	1.424	0.217	395	410	926

Table S2. Detailed absorption and emission peaks of TPA-An-Ph in different solvents

solvents	ε	n	$f(\varepsilon,n)$	λ_a [nm]	λ_f [nm]	ν_a-ν_f [cm^{-1}]
hexane	1.90	1.375	0	393	433	2350
toulene	2.40	1.497	0.013	396	449	2981
triethylamine	2.42	1.401	0.048	394	440	2653
isopropyl ether	3.88	1.386	0.145	393	449	3174
chloroform	4.80	1.446	0.148	397	460	3450
ethyl acetate	5.10	1.372	0.200	394	468	4013
tetrahydrofuran	7.58	1.407	0.210	395	469	3995
dichloromethane	8.93	1.424	0.217	396	494	5010

Table S3. Detailed absorption and emission peaks of TPA-An-mPhCz in different solvents

solvents	ε	n	$f(\varepsilon,n)$	λ_a [nm]	λ_f [nm]	ν_a-ν_f [cm^{-1}]
hexane	1.90	1.375	0	393	437	2562
toulene	2.40	1.497	0.013	397	456	3259
triethylamine	2.42	1.401	0.048	395	448	3124
isopropyl ether	3.88	1.386	0.145	393	453	3370
chloroform	4.80	1.446	0.148	397	476	4181
ethyl acetate	5.10	1.372	0.200	394	472	4194
tetrahydrofuran	7.58	1.407	0.210	396	476	4244
dichloromethane	8.93	1.424	0.217	397	496	5028

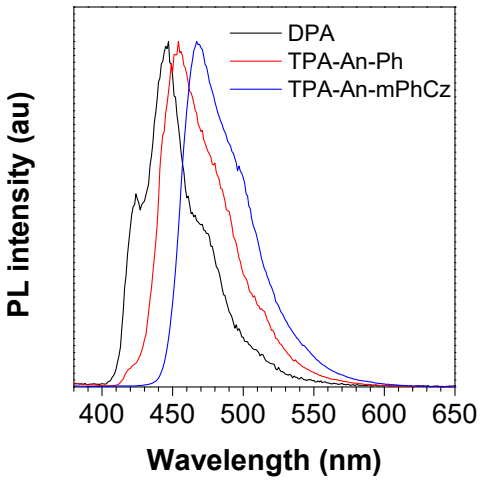

Fig. S3. PL spectra of the films of DPA, TPA-An-Ph and TPA-An-mPhCz at 77 K. λ_{ex}: 360 nm.

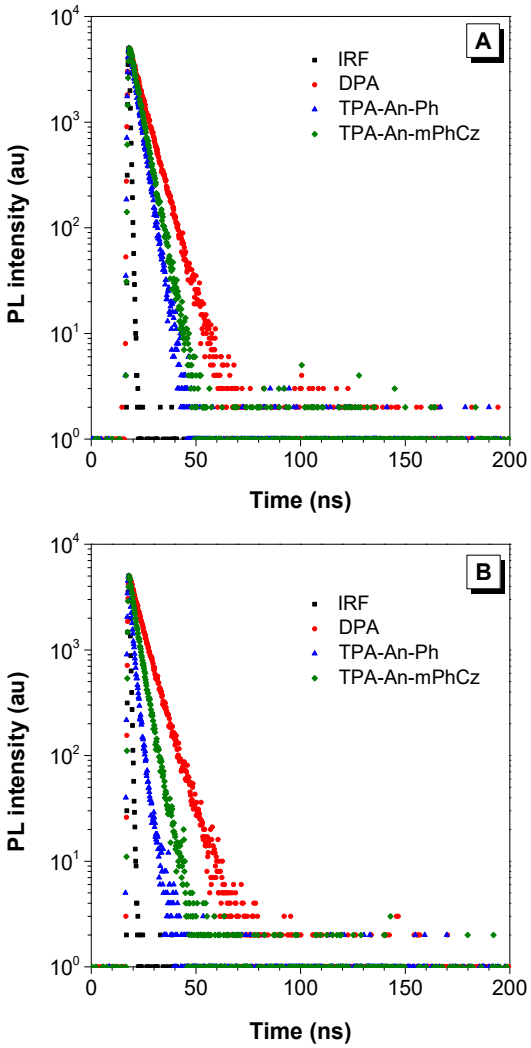

Fig. S4. PL lifetime decays of DPA, TPA-An-Ph and TPA-An-mPhCz (A) in THF solutions (concentration: 10 μM) and (B) film state. λ_{ex}: 360 nm.

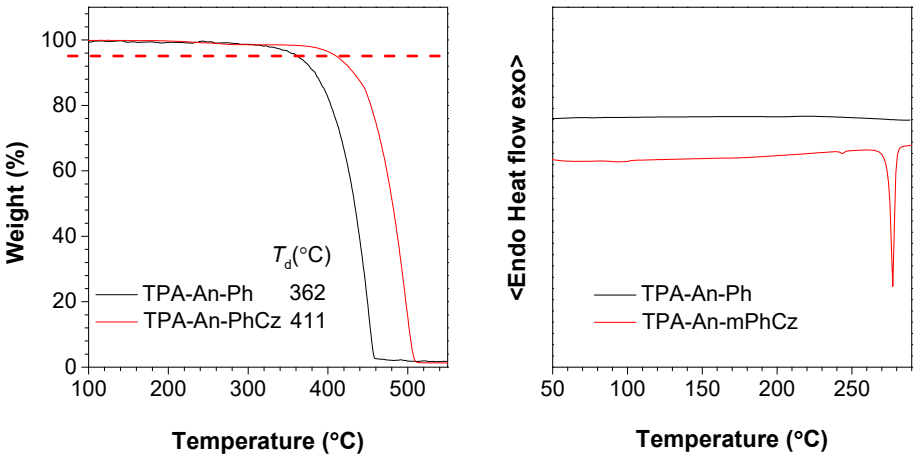

Fig. S5. TGA thermograms (left) and DSC curve (right) of TPA-An-Ph and TPA-An-mPhCz, recorded under nitrogen at a heating rate of 10 °C/min.

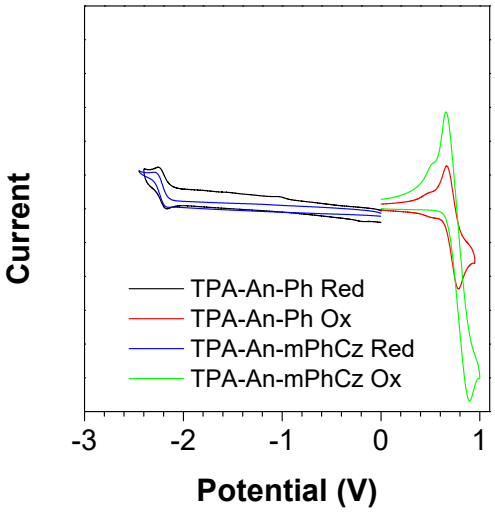

Fig. S6. Cyclic voltammograms of TPA-An-Ph and TPA-An-mPhCz, measured in dichloromethane containing 0.1 M tetra-*n*-butylammonium hexafluorophosphate.

Table S4. Photophysical, thermal and electronic properties of TPA-An-Ph and TPA-An-mPhCz

compounds	λ_{abs}[a] [nm] sol	λ_{PL} [nm] sol[a] /film[b]	Φ_{PL}[c] [%] sol[a] /film[b]	τ[d] [ns] sol[a] /film[b]	T_d [°C]	T_g [°C]	HOMO/LUMO[e] [eV]
TPA-An-Ph	360	469/460	30.0/40.1	3.45/1.95	362	-	-5.20/-2.51
TPA-An-mPhCz	360	478/470	57.8/65.1	3.85/3.58	411	-	-5.22/-2.52

[a] Measured in oxygen-free THF solution at room temperature (10^{-5} M). [b] Measured in thin film. [c] The absolute PL quantum yield. [d] PL lifetimes at room temperature under air conditions. [e] Measured by cyclic voltammetry.

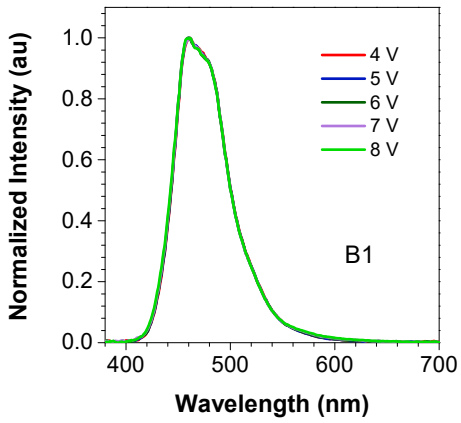

Fig. S7. Electroluminescence (EL) spectra of device B1 at various voltages.

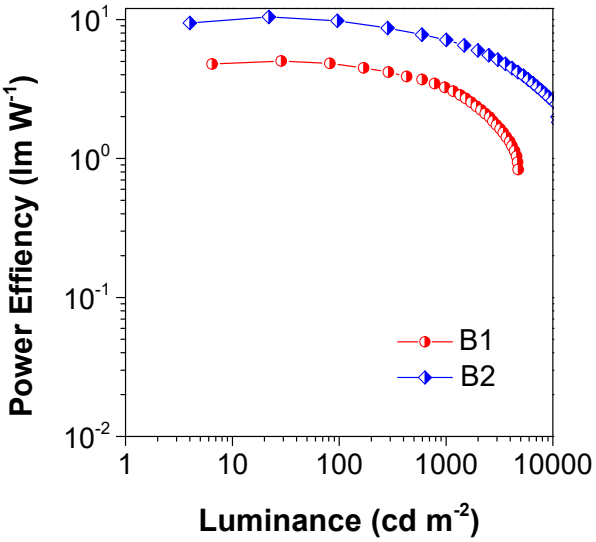

Fig. S8. Power efficiency versus luminanc curves of the non-doped OLEDs using TPA-An-Ph and TPA-An-mPhCz as EMLs.

Table S5. EL performance of TPA-An-Ph and TPA-An-mPhCz based non-doped devices

device	V_{on}(V)	L_{max}(cd/m^2)	CE[a)](cd/A)	PE[a)](lm/W)	EQE[a)](%)	λ_{max}[b)](nm)	CIE (x, y)[b)]
B1	3.2	4737	5.54/4.86	5.02/3.05	4.51/4.02	460	(0.14, 0.16)
B2	3.0	13335	10.62/9.09	10.42/7.14	8.10/6.97	470	(0.14, 0.17)

[a)] Order of maximum, then values at 1000 cd m^{-2}; [b)] Measured at 1000 cd m^{-2}. Device configuration: ITO/HAT-CN (5 nm)/TAPC (60 nm)/TCTA (5 nm)/EML (20 nm)/TmPyPB (40 nm)/LiF (1 nm)/Al. Devices B1 and B2 refer to the EMLs of TPA-An-Ph and TPA-An-mPhCz, respectively.

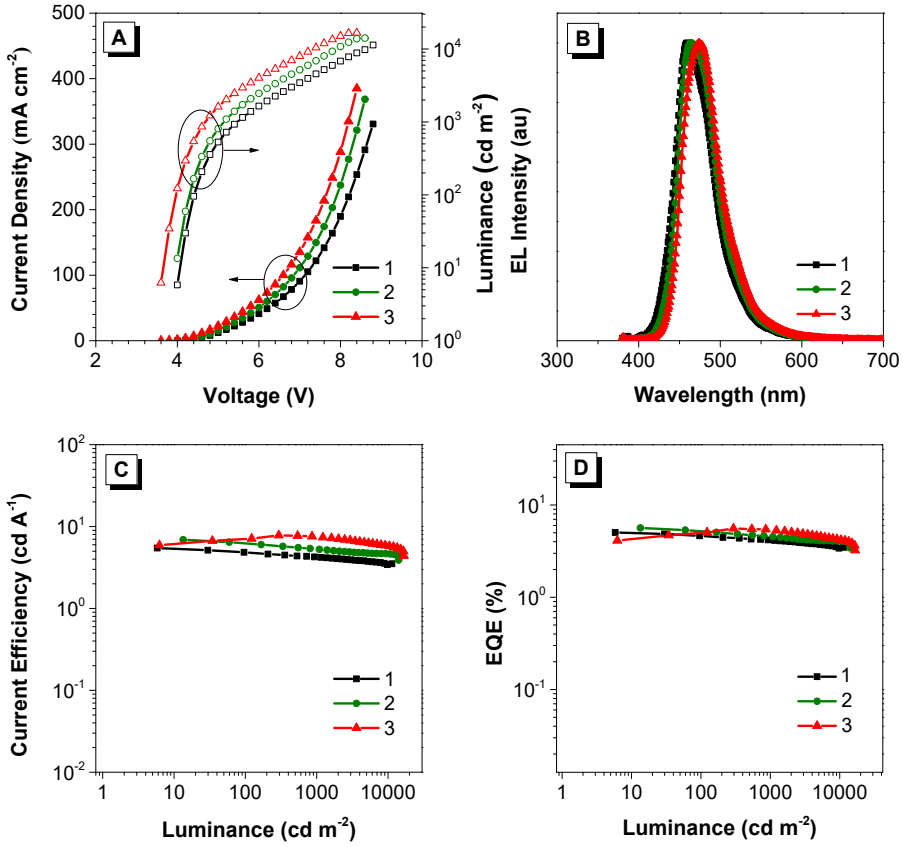

Fig. S9 (A) Current density-voltage-luminance (J-V-L) characteristics of TPA-An-mPhCz-based doped devices 1-3. (B) Electroluminescence (EL) spectra of TPA-An-mPhCz-based doped devices 1-3. at various voltages. (C) CE and (D) EQE versus luminance curves of t TPA-An-mPhCz-based doped devices 1-3. Device configuration: ITO/HAT-CN (5 nm)/TAPC (60 nm)/TCTA (5 nm)/EML (20 nm)/TmPyPB (40 nm)/LiF (1 nm)/Al; Device 1: EML: 26DCZPPy:TPB-An-mphCz 10%; Device2: EML: 26DCZPPy:TPB-An-mphCz 20%; Device3: EML: 26DCZPPy:TPB-An-mphCz 50%.

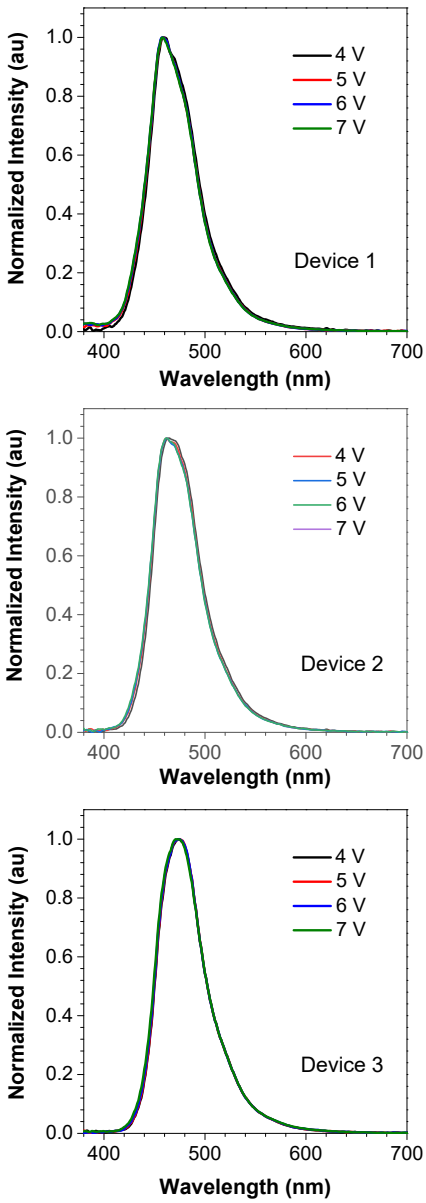

Fig. S10 EL spectra of TPA-An-mPhCz-based doped devices 1-3 at various voltages.

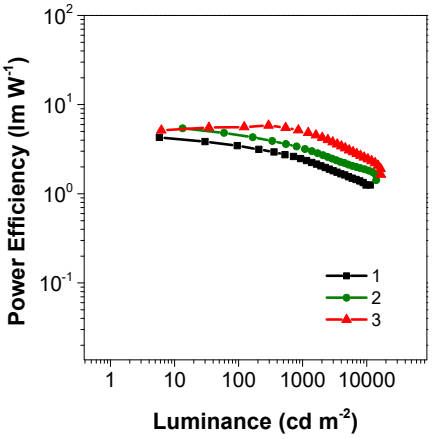

Fig. S11. Power efficiency versus luminanc curves of the TPA-An-mPhCz-based doped OLEDs

Table S6. EL performance of TPA-An-mPhCz based doped devices

device	V_{on}(V)	L_{max}(cd/m^2)	CE[a)](cd/A)	PE[a)](lm/W)	EQE[a)](%)	λ_{max}[b)](nm)	CIE (x, y)[b)]
1	4.0	11363	5.47/4.20	4.29/2.36	5.04/4.13	458	(0.14, 0.12)
2	4.0	14092	6.90/5.26	5.42/3.18	5.60/4.50	462	(0.14, 0.14)
3	3.8	16692	7.82/7.39	5.85/4.83	5.60/5.30	474	(0.14, 0.19)

[a)] Order of maximum, then values at 1000 cd m^{-2}; [b)] Measured at 1000 cd m^{-2}. Device configuration: ITO/HAT-CN (5 nm)/TAPC (60 nm)/TCTA (5 nm)/EML (20 nm)/TmPyPB (40 nm)/LiF (1 nm)/Al; Device 1: EML: 26DCZ:TPB-An-mphCz 10%; Device2: EML: 26DCZ:TPB-An-mphCz 20%; Device3: EML: 26DCZ:TPB-An-mphCz 50%.

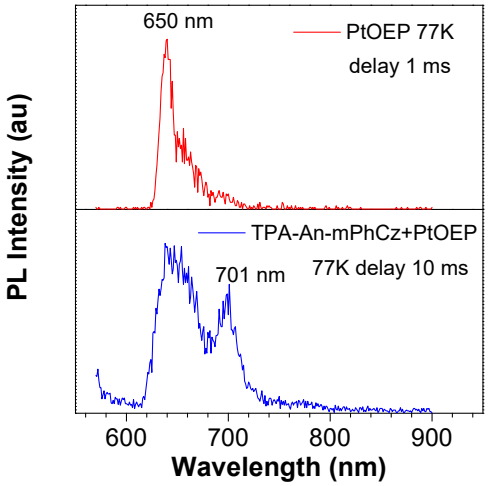

Fig. S12. Upper: the phosphorescence of Platinum octaethylporphyrin (PtOEP) in THF at 77 K, excited by 550 nm; lower: the phosphorescence of TPA-An-mPhCz in THF at 77 K, excited by 550 nm, measured in a mixture of PtOEP (10^{-4} M) + TPA-An-mPhCz (10^{-4} M) in THF.

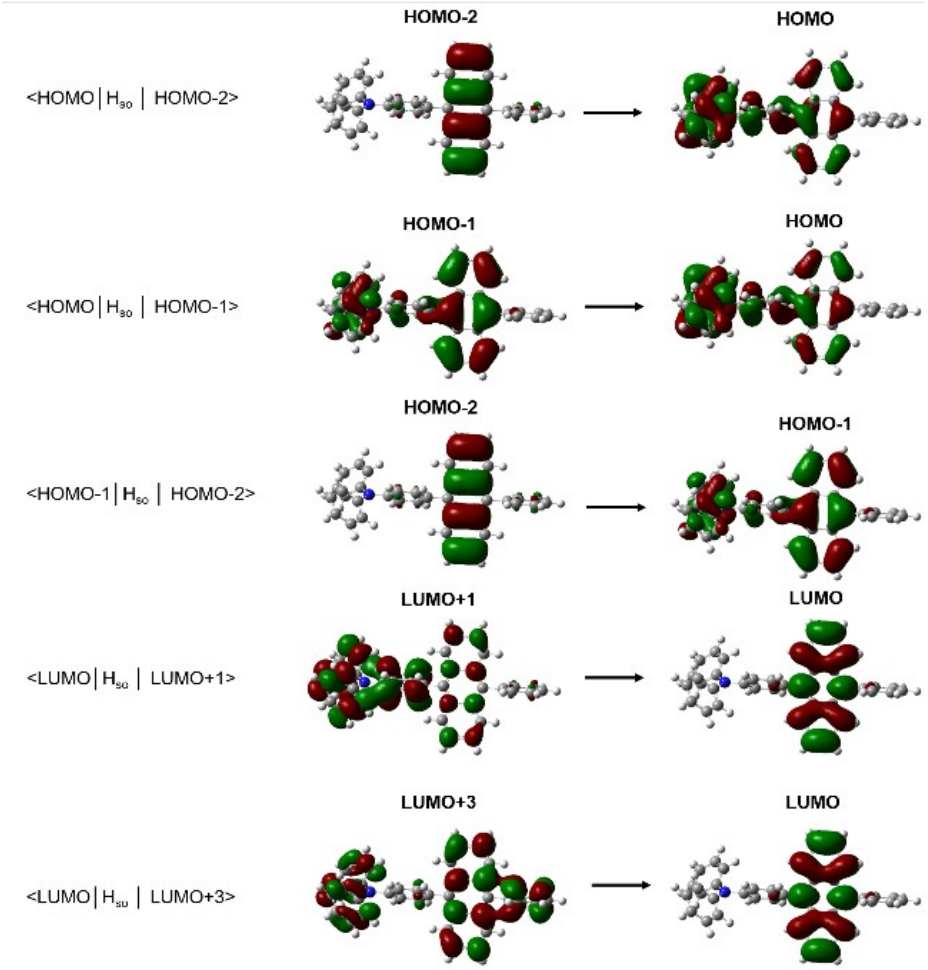

Fig. S13. Possible TTU transitions of TPA-An-Ph. Molecular orbitals related to TTU transitions from ^{3}(TT) to S_n in TPA-An-Ph.

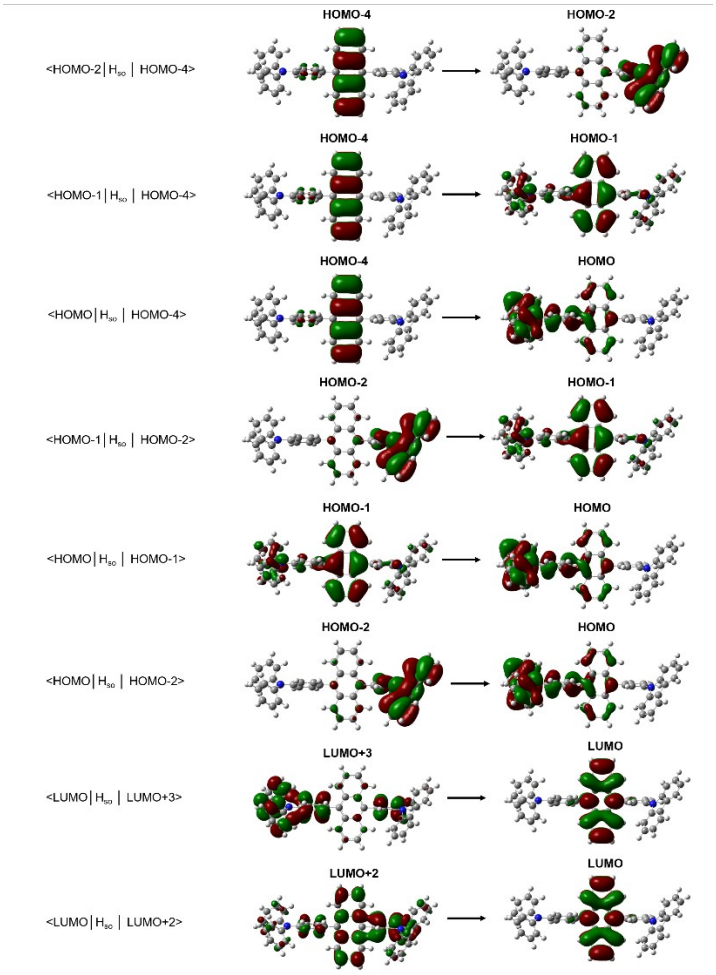

Fig. S14. Possible TTU transitions of TPA-An-mPhCz. Molecular orbitals related to TTU transitions from ^{3}(TT) to S_n in TPA-An-mPhCz.

Table S7. Electronic transitions calculated by B3LYP/6-311G(d,p) of S_n with energies lower than twice the T_1 energy (~3.46 eV) and T_m with energies in the range of 3.4-3.50 eV

compounds	state	energy (eV)	transition	percentage contribution (%)
TPA-An-Ph	S_1	2.8923	HOMO→LUMO	96.77
	S_2	3.1209	HOMO-1→LUMO	95.75
	T_7	3.4232	HOMO-2→LUMO	36.22
			HOMO-1→LUMO+1	24.15
			HOMO-1→LUMO+3	10.67
			HOMO→LUMO+3	17.83
TPA-An-mPhCz	S_1	2.8304	HOMO→LUMO	98.39
	S_2	3.1025	HOMO-1→LUMO	96.21
	S_3	3.1876	HOMO-2→LUMO	98.39
	T_{10}	3.4206	HOMO-4→LUMO	34.45
			HOMO-1→LUMO+2	27.92
	T_{11}	3.4610	HOMO-2→LUMO+2	30.39
			HOMO-2→LUMO+3	11.94

Table S8. Spin-orbit matrices related to possible TTU transitions from ^{3}(TT) to Sn for the anthracene derivatives

compound	transition	SOC matrix		related molecular orbitals
TPA-An-Ph	$^3T_1T_1 \rightarrow S_1$	$<S_1 \mid H_{so} \mid T_7>$	<HOMO | Hso | HOMO-2>	Figure S10
			<HOMO | Hso | HOMO-1>	
			<LUMO | Hso | LUMO+1>	
			<LUMO | Hso | LUMO+3>	
	$^3T_1T_1 \rightarrow S_2$	$<S_2 \mid H_{so} \mid T_7>$	<HOMO-1 | Hso | HOMO-2>	
TPA-An-mPhCz	$^3T_1T_1 \rightarrow S_1$	$<S_1 \mid H_{so} \mid T_{10}>$	<HOMO | Hso | HOMO-4>	Figure S12
			<HOMO | Hso | HOMO-1>	
			<LUMO | Hso | LUMO+2>	
		$<S_1 \mid H_{so} \mid T_{11}>$	<HOMO | Hso | HOMO-2>	
			<LUMO | Hso | LUMO+3>	
	$^3T_1T_1 \rightarrow S_2$	$<S_2 \mid H_{so} \mid T_{10}>$	<HOMO-1 | Hso | HOMO-4>	
		$<S_2 \mid H_{so} \mid T_{11}>$	<HOMO-1 | Hso | HOMO-2>	
	$^3T_1T_1 \rightarrow S_3$	$<S_3 \mid H_{so} \mid T_{10}>$	<HOMO-2 | Hso | HOMO-4>	

Reference

[1] S. Tao, Y. Zhou, C. Lee, S. Lee, D. Huang and X. Zhang, *J. Phy. Chem. C* 2008, **112**, 14603-14606.